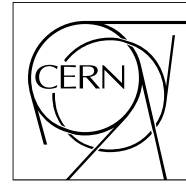


The Compact Muon Solenoid Experiment

CMS Note

Mailing address: CMS CERN, CH-1211 GENEVA 23, Switzerland



21 January 2008

Lorentz angle calibration for the barrel pixel detector

L. Wilke^{1),2)}, V. Chiochia¹⁾, T. Speer^{1),3)}

1) Physik Institut, Universität Zürich, Switzerland

2) Paul Scherrer Institut, Villigen, Switzerland

3) now Brown University, USA

Abstract

A method to measure the Lorentz angle in the barrel pixel detector of CMS is presented. This measurement from CMS data will be necessary during operation since the electric field in the sensors will change with increasing irradiation. The approach described in this note uses well measured muon tracks to determine the drift of the electrons in the pixel sensors. From an analysis of simulated data an accuracy of 2% on θ_L can be achieved from just 1000 muon tracks. This corresponds to a systematic shift in the hit reconstruction of less than $1.5 \mu\text{m}$ which will decrease with increasing integrated luminosity.

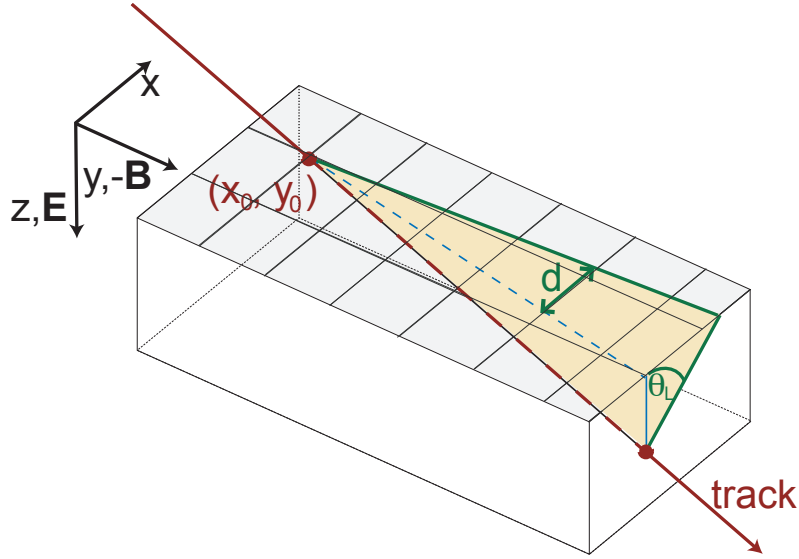


Figure 1: A sketch of a track passing through the pixel sensor. The plane of the charge carriers drift is shaded. The Lorentz angle is labelled as θ_L

1 Introduction

The CMS pixel detector [1] is located inside a 4 T superconducting solenoid. The barrel pixel detector consists of three layers, with radii of 4.3 cm, 7.2 cm, and 11 cm. The layers are composed of modular detector units consisting of thin, segmented silicon sensors with highly integrated readout chips. The sensors are mounted on a ladder like support structure along the beam-pipe direction which is then installed on two half cylinders. Electron-hole pairs produced by charged particles traversing the pixel sensors will thus experience the Lorentz force and drift under the combined magnetic and electric fields (see Fig. 1). This enhances charge sharing between pixels and improves the spatial resolution through charge interpolation. This is possible due to an analog readout and a noise level which is very low relative to the signal.

During LHC operation, radiation damage will change the properties of the silicon sensors. The increasing number of defects caused by incident particles interacting with silicon lattice atoms impacts the Lorentz angle in several ways [1]. Trapping of charge carriers leads to a reduction of the collected charge which has to be compensated by a higher bias voltage, leading to a reduced Lorentz deflection [2]. The spatial resolution depends, among other factors, on the knowledge of the Lorentz deflection. Test beam studies have shown that the Lorentz angle at 4 T varies from 23° for an unirradiated sensor to 8° for a highly irradiated sensor due to the necessary increase in bias voltage from 150 V to 600 V (see Fig. 2(a), [2]). Furthermore, the initially uniform electric field across the sensor bulk will change and the linear correlation between drift length and depth in the sensor bulk will no longer be valid (see Fig. 2(b), [3]).

In this note a strategy to extract the drift length as a function of the depth in the silicon bulk is presented. From this the Lorentz angle can be extracted. The study was performed with the CMS simulation and reconstruction software (CMSSW [4], version 1.6.0). Unless otherwise stated, this study was performed using simulated single muon events with a Lorentz angle set to 23° , corresponding to non irradiated sensors at 150 V. Muon events were produced with a transverse momentum of 10 GeV/c and were randomly distributed in the pseudorapidity range $|\eta| < 2.5$. The primary vertex was smeared along the beamline with a Gaussian distribution with $\sigma = 5.3$ cm.

As shown in Fig. 3, each layer is segmented into eight rings along the beam direction. The irradiation of each readout unit depends on the distance to the interaction point, but should be independent of the azimuth angle. In this note the Lorentz angle will thus be measured for each of the eight rings in the 3 barrel layers.

The note is structured as follows: in Section 2 we describe the measurement technique and present the results; in Section 3 different systematic studies are described. Conclusions are given in Section 4.

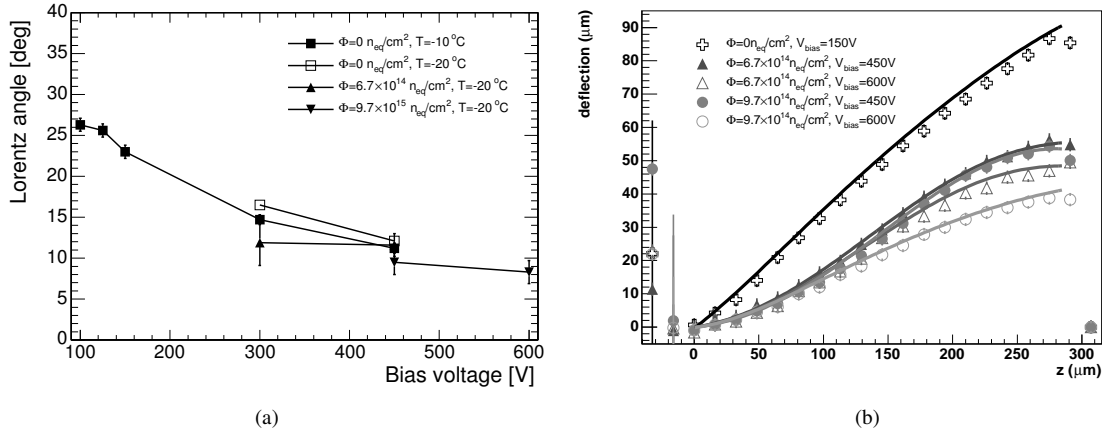


Figure 2: (a) The Lorentz angle measured with sensors irradiated to different fluences as function of the bias voltage. Measurements are performed at different temperatures and shown for a 4 T magnetic field. At early stage a bias voltage of 150 V is applied resulting in a Lorentz angle of $\theta_L = 23^\circ$. For high irradiation fluences the bias voltage has to be increased to 600 V to compensate trapping of charge carriers. The resulting Lorentz angle is 8° [2]. (b) Charge carriers deflection (drift length) measured as a function of depth in the silicon bulk (markers) compared to a simulation (solid lines) for different bias voltages and irradiation fluences. For the unirradiated case the correlation is approximately linear. For irradiated sensors the correlation is not linear due to the doubly peaked electric field profile [3].

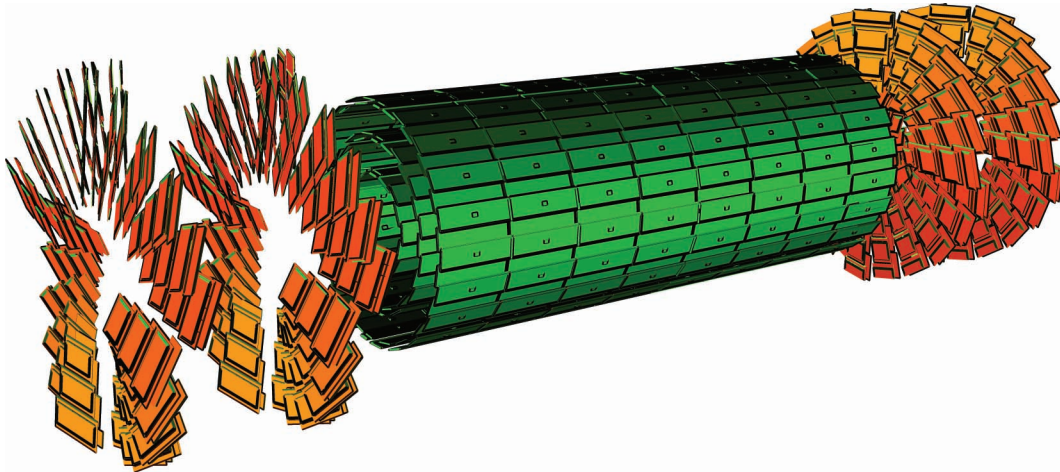


Figure 3: Sketch of the CMS forward and barrel pixel detectors. The barrel pixel detector consists of the three central layers.

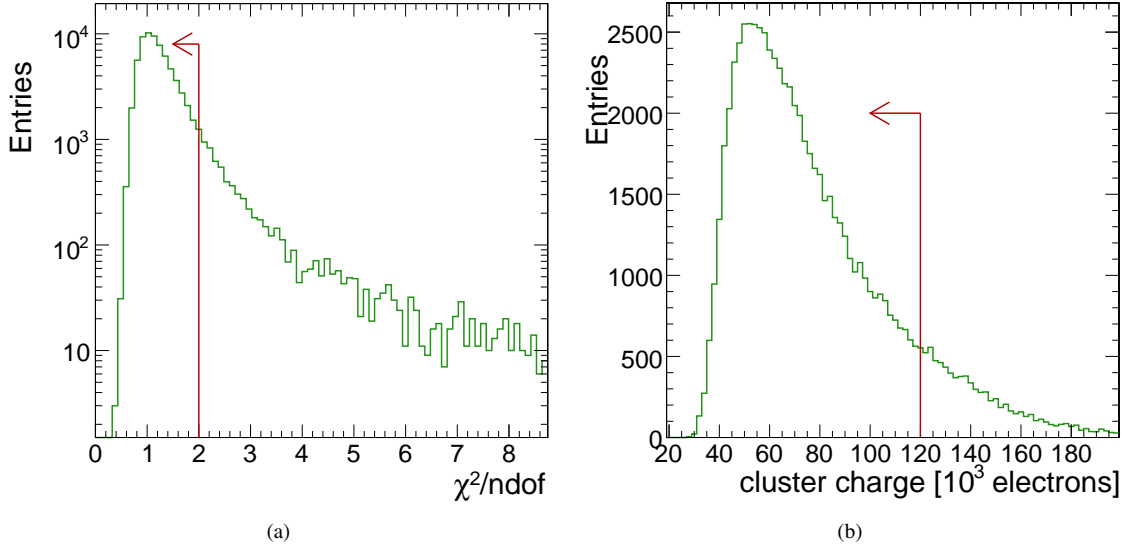


Figure 4: (a) χ^2/ndof for the track fit. To assure a correct reconstruction it is required that $\chi^2/\text{ndof} < 2$. (b) Charge deposited by a 10 GeV/c muon track which crosses the pixel ring placed at $\eta = 2$. To avoid cluster distortion from secondary electrons, the charge is required to be less than 120 000 electrons.

2 Measurement of the Lorentz angle

The measurement of the Lorentz angle is based on the grazing angle technique described in [5]. In principle, all types of tracks would be suitable for the measurement. Due to the clean reconstruction of muons it was decided that only these would be used. Events for the measurement of the Lorentz angle are selected as follows:

- *Track selection:* Tracks associated with segments in the muon chambers are tagged as muon tracks. The muon reconstruction is described in [6]. Muon tracks are required to have a minimum transverse momentum of 3 GeV/c and a reduced χ^2 of less than two (see Fig. 4(a)).
- *Cluster selection:* In order to measure the drift length as a function of depth, only tracks with shallow impact angle with respect to the local y axis (i.e. small β in Fig. 5) are used, which corresponds to tracks with a high pseudorapidity. Pixel hits in the muon track are therefore required to contain at least four pixels above threshold along the local y direction. Furthermore, to ensure the correct hit reconstruction and to avoid satellite clusters due to secondary electrons the total cluster charge has to be less than 120 000 electrons (see Fig. 4(b)).

The impact position is measured by extrapolating the trajectory to each detector layer. The charge collected in the pixel sensor is shown as a function of the distance to the impact position in Fig. 6(a), with Δx and Δy defined as:

$$\Delta x = x - x_0, \quad (1)$$

$$\Delta y = y - y_0, \quad (2)$$

where (x_0, y_0) is the track impact position on the surface of the pixel which is bump-bonded to the readout chip and (x, y) is the position of the pixel centre. Now the drift of the electrons depending on the depth in which they were produced has to be calculated. The impact angles in of the track (Fig. 5) are defined as

$$\tan \alpha = \frac{p_z}{p_x}, \quad (3)$$

$$\tan \beta = \frac{p_z}{p_y}, \quad (4)$$

$$\tan \gamma = \frac{p_x}{p_y}, \quad (5)$$

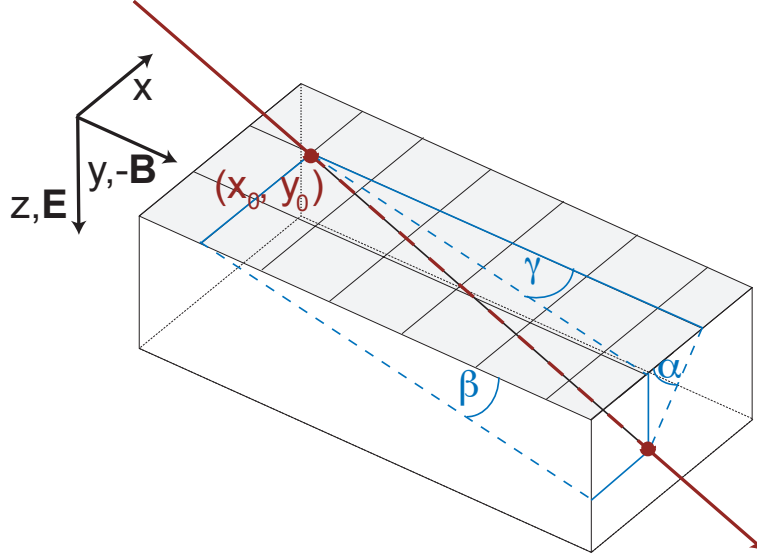


Figure 5: A sketch defining the three angles of a track with respect to the detector.

where p_x , p_y , and p_z are given in the local coordinate system. One can then calculate the drift distance d due to the magnetic field and the production depth of the electrons:

$$d = \Delta x - \Delta y \cdot \tan \gamma , \quad (6)$$

$$z = \Delta y \cdot \tan \beta . \quad (7)$$

Without a magnetic field, the direction of the clusters largest extension is parallel to the track projection on the (x, y) plane, which does not vary more than 10° from the x -direction for a 10 GeV/ c muon. The width of the charge distribution is given by the pixel pitch along x (100 μm) while its length is given by $z / \tan \beta$.

Combining the information from a large number of tracks, the charge drift distance vs. depth is determined (Fig. 6). The Lorentz angle is equal to the slope of this distribution. The average drift distance of an electron created at a certain depth is obtained from Fig. 6(b). A linear fit is performed over the total depth of the detector excluding the first and last 50 μm where the charge drift is systematically displaced by the finite size of the pixel cell (Fig. 7(a)).

Since the irradiation will not be uniform across the detector the Lorentz angle has to be determined independently for different regions of pseudorapidity. The barrel pixel detector is subdivided into three layers, which are further subdivided into eight rings, corresponding to the eight modules along the direction of the beam-pipe. The fit results for an assumed Lorentz angle of 23° in the simulation are shown in Fig. 7(b). The results match the assumed value to an accuracy of 2% although the two central rings (4,5) in the outermost layer clearly require more statistics. Due to the requirement of the shallow angle with the detector, only tracks which are highly displaced from the nominal interaction point (≈ 15 cm) can be used here, resulting in a smaller track sample.

3 Systematic studies

In this section, possible sources of systematic uncertainties impairing the Lorentz angle measurement are investigated.

First, the dependence of the relative uncertainty of the Lorentz angle measurement on the number of tracks used is examined. As shown in Fig. 8(a), the relative uncertainty of $\tan \theta_L$ is inversely proportional to the square root of the number of tracks. To achieve a relative uncertainty of 2%, approximately 1000 tracks are needed in the corresponding ring. For a Lorentz angle of 23° , this corresponds to an uncertainty of less than 0.5° and a displacement of 1.14 μm .

To maximise the number of muon tracks, the minimum transverse momentum of the muons used should be set

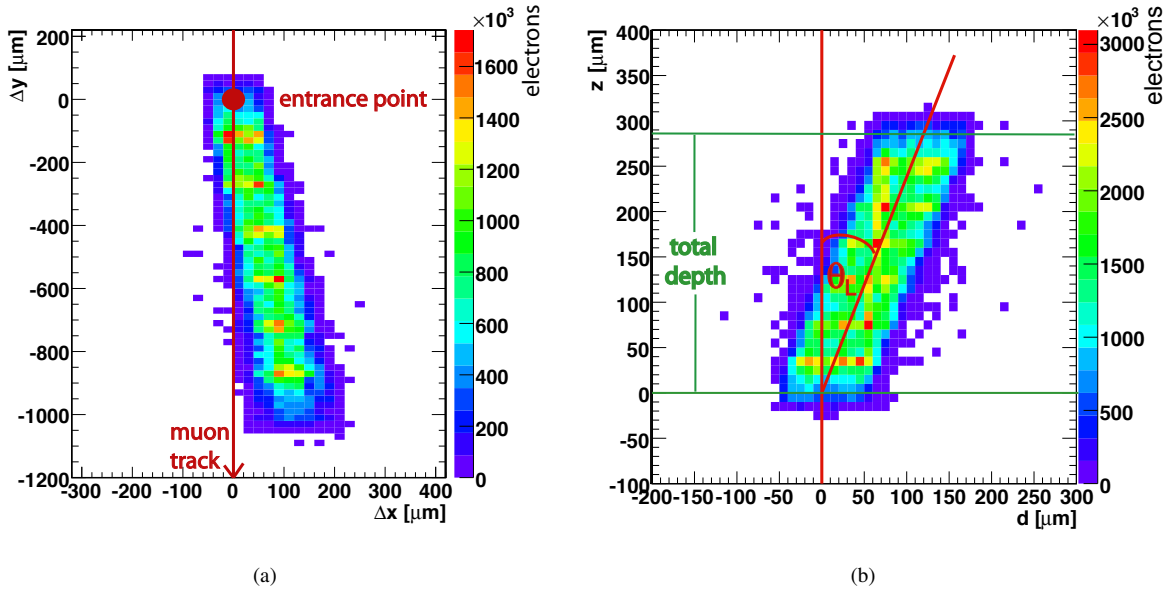


Figure 6: (a) Pixel charge distribution as a function of distance to the track impact position in x and y . (b) Depth in which the electrons were produced versus their drift distance. Both figures are for muon tracks which cross the pixel ring placed at $\eta = 2$.

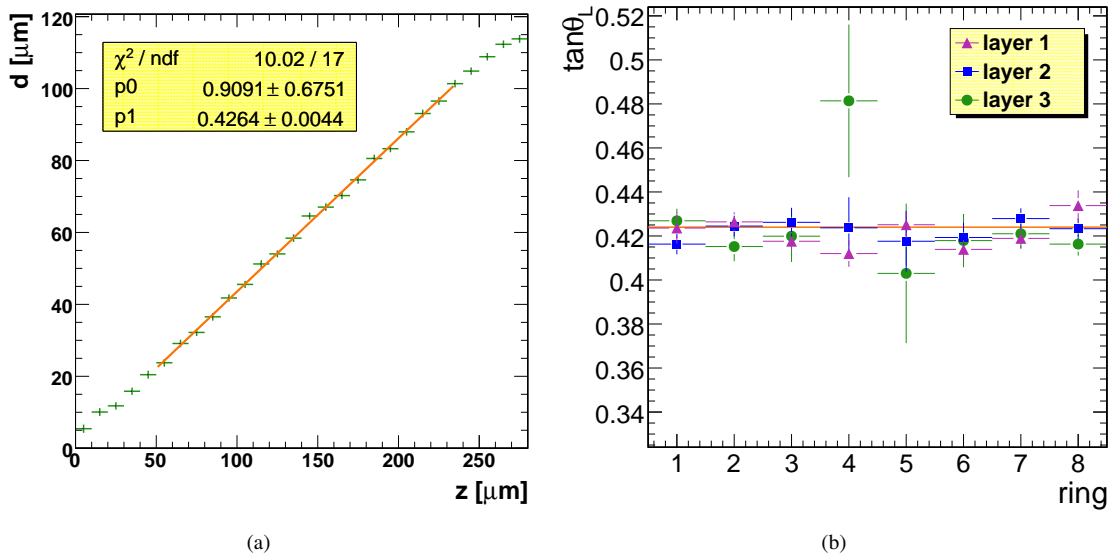


Figure 7: (a) The average drift of electrons as a function of the production depth in the silicon sensor bulk. The solid line shows the fit. The slope, $p1$, corresponds to $\tan \theta_L$. (b) The results for $\tan \theta_L$ for the three barrel layers and eight detector rings. The solid line shows the simulated value of $\tan \theta_L = 0.424$ corresponding to $\theta_L = 23^\circ$.

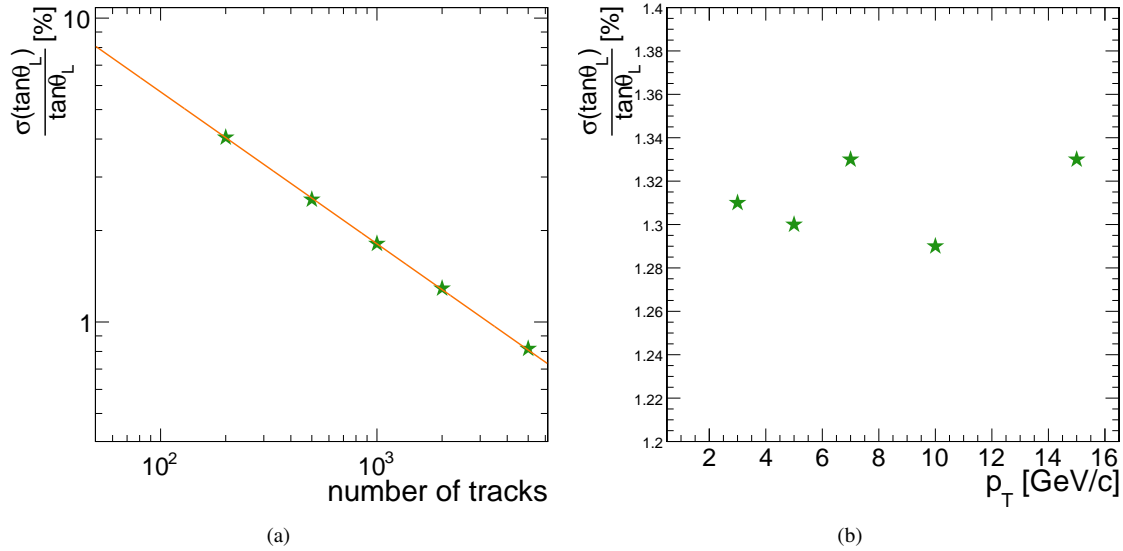


Figure 8: (a) Relative uncertainty of $\tan\theta_L$ as function of the number of tracks. Solid stars show the measurement while the line shows a fit. The relative uncertainty is inversely proportional to the square root of the number of tracks, as expected. As shown in Fig.(b), the $\tan\theta_L$ relative uncertainty is independent of the transverse muon momentum down to 3 GeV/c; hence all muons with $p_T > 3$ GeV/c can be used for the fit.

as low as possible. We investigated whether multiple scattering would increase the relative uncertainty for low momentum muons. The Lorentz angle is measured for generated single muon samples with different momenta. As shown in Fig. 8(b), there is no dependence of the relative uncertainty of $\tan\theta_L$ on the transverse momentum down to 3 GeV/c as well as no bias on the measurement. Based on this result, reconstructed muons with a minimum transverse momentum of 3 GeV/c are used for the measurement of the Lorentz angle.

3.1 Different values of the Lorentz angle

Since the Lorentz angle decreases with increasing bias voltage, the measurable drift length will be smaller. To determine whether smaller Lorentz angles can be measured the method was applied to data with Lorentz angles set to 15° and 8° . Fig. 9 shows the results; the absolute uncertainty of the measurement is not changed with respect to the measurement of $\theta_L = 23^\circ$.

Furthermore the influence of a wrong Lorentz angle assumption to the reconstruction is studied. A sample of events simulated with $\theta_L = 23^\circ$ in the barrel pixel detector is reconstructed assuming a value of $\theta_L = 18^\circ$, which implies a systematic shift of 15 μm in the measured pixel hit x -position. All other parameters in the simulation and reconstruction are kept ideal. The measured Lorentz angle agrees with the simulated value of $\theta_L = 23^\circ$ and is not biased by the wrong value assumed in the pixel hit reconstruction (see Fig. 10).

3.2 Tracker misalignment studies

Results presented in Section 2 are obtained with a perfectly aligned tracker. To investigate the sensitivity of the method to misalignment the study is repeated using an alignment scenario corresponding to an integrated luminosity of 10 pb^{-1} . In this alignment scenario an educated guess is made on how well the position of the detectors will be known after taking data for a luminosity of 10 pb^{-1} . The position uncertainty of the sensors, ladders, and half cylinders is assumed to be 60 μm , 10 μm , and 10 μm , respectively. Two sets of simulated Drell-Yan events are used: one sample is reconstructed assuming perfect alignment while the second is reconstructed with the misaligned scenario. Fig. 11 shows the results. The measured values agree with the simulation in both cases and the achieved precision is roughly 0.5% for most rings, reaching 4% for the outermost central rings, using a total of about 400 000 events.

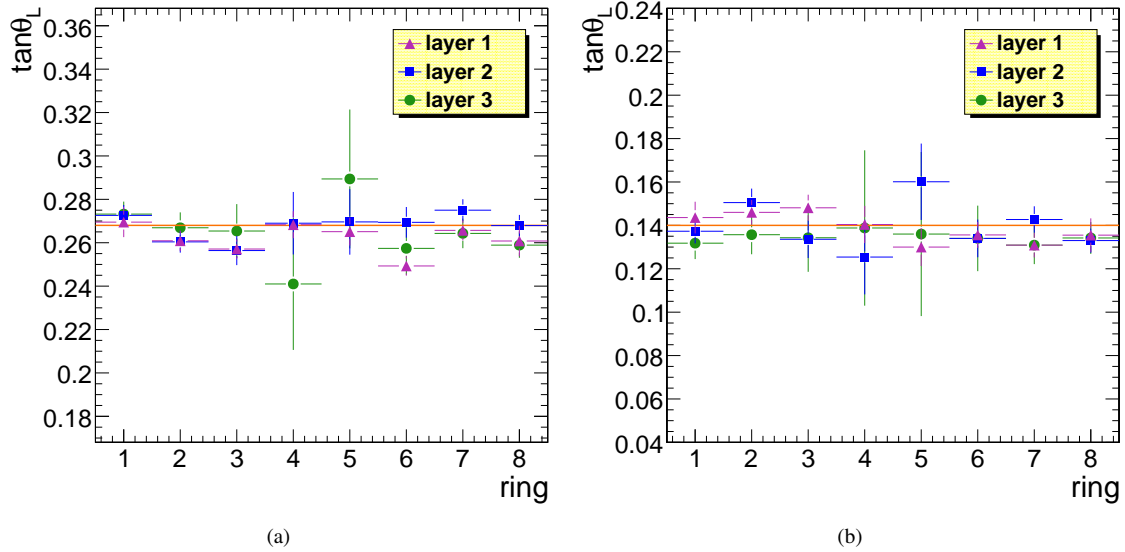


Figure 9: The results for $\tan \theta_L$ for the three layers and eight detector rings for an input value of $\tan \theta_L = 0.268$, corresponding to $\theta_L = 15^\circ$ (a) and $\tan \theta_L = 0.140$, corresponding to $\theta_L = 8^\circ$ (b).

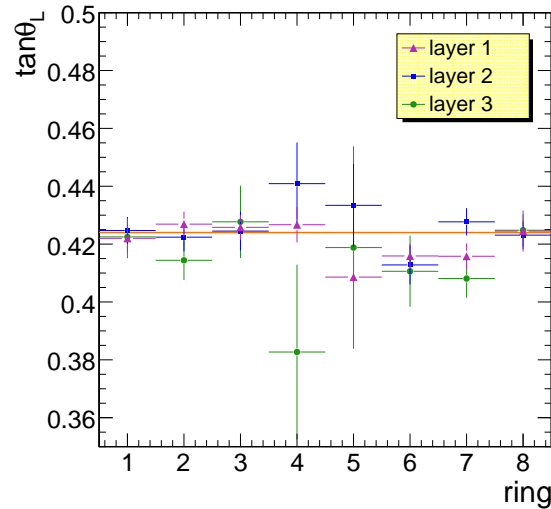


Figure 10: $\tan \theta_L$ measured for the three layers as a function of the detector ring. The solid line shows the simulated value of $\tan \theta_L = 0.424$ corresponding to $\theta_L = 23^\circ$. A wrong Lorentz angle of $\tan \theta_L = 0.320$ corresponding to $\theta_L = 18^\circ$ was assumed in the reconstruction.

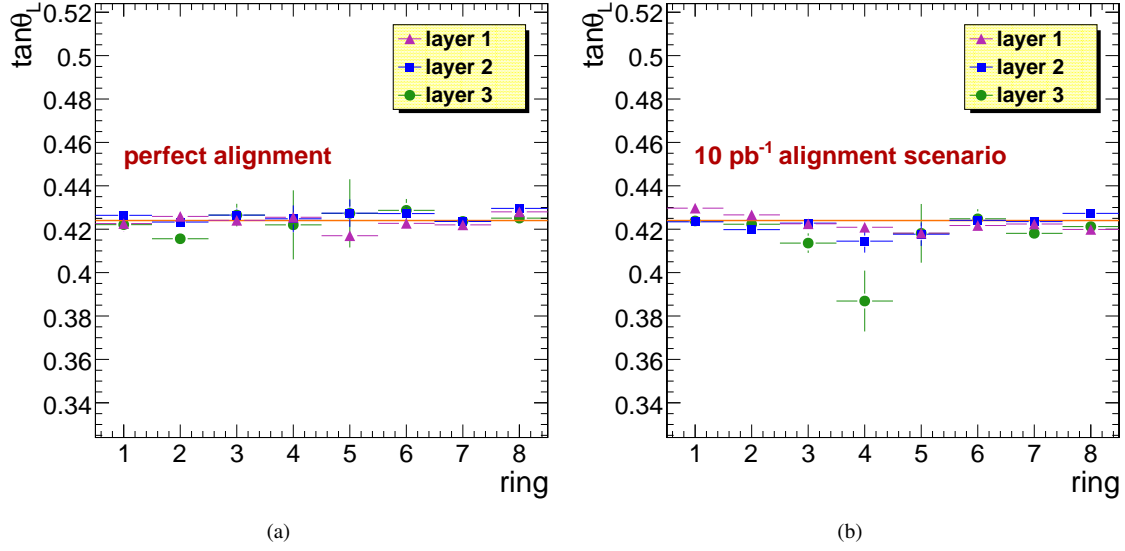


Figure 11: Measured $\tan \theta_L$ for each of the three layers as a function of the detector ring. Simulated Drell Yan events are reconstructed for a perfectly aligned detector (a) and for the 10 pb⁻¹ alignment scenario (b).

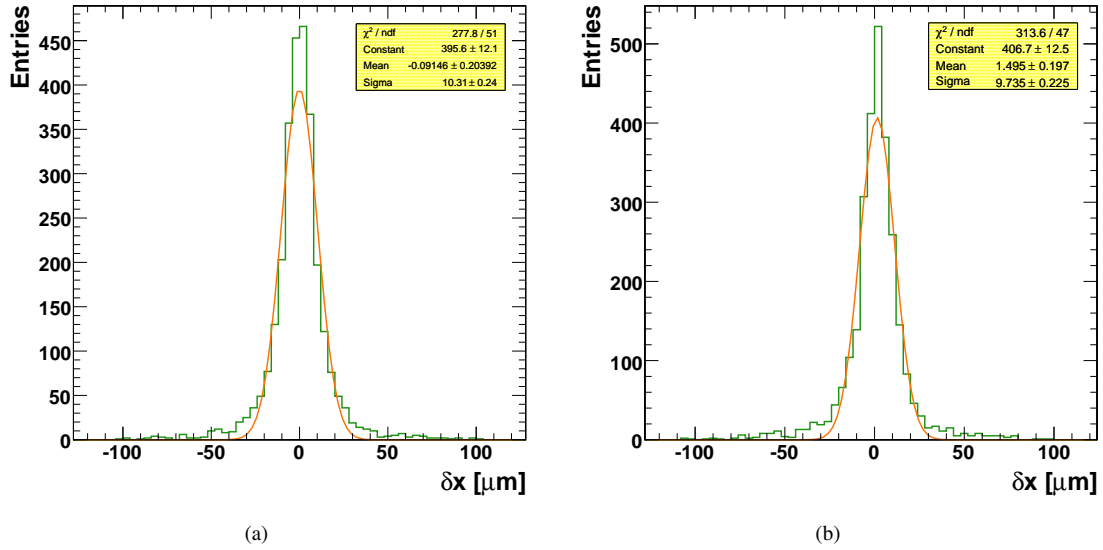


Figure 12: Residuals of reconstructed hits in the x -direction. In (a) for the correct Lorentz angle, in (b) for a Lorentz angle of 22.6° instead of 23°, resulting in a shift of 1.5 μm .

3.3 Impact of wrong Lorentz angle on hit resolution

An error of the Lorentz angle used for the reconstruction of hits will lead to a systematic shift in the hit position. The reconstructed x -position will be shifted by

$$\delta x = \delta [\tan \theta_L] \cdot \bar{z}, \quad (8)$$

where $\delta [\tan \theta_L]$ is the error of $\tan \theta_L$ and \bar{z} is the mean depth of charge carrier production. An error of 2% on $\tan \theta_L$, leads to a shift of 1.14 μm . To verify this, the shift was measured on a sample of generated single muon events by setting $\tan \theta_L$ in the reconstruction 2% lower than in the simulation, namely to $\theta_L = 22.6^\circ$. As shown in Fig. 12 the measured shift is 1.5 μm , close to the expected value. The width of the distribution is not changed. The shift is significantly smaller than the position resolution. The alignment procedure of the pixel detector should absorb this shift because it will not be possible to distinguish between a shift of a detector module and the shift due to the Lorentz angle.

4 Conclusions

A method to measure the Lorentz angle in the barrel pixel detector with muon tracks was developed. Due to the nonuniform irradiation the measurement is performed for different positions along the beam-pipe direction and for the three layers of the pixel barrel detector independently. This method offers the possibility to measure the Lorentz angle with a precision of 2% (i.e. 0.5°) using only 1000 tracks for a pixel detector ring. This will lead to a shift of $1.5\ \mu\text{m}$ in the x -direction which is much smaller than the hit resolution of $10\ \mu\text{m}$. For a larger number of muon tracks used in the Lorentz angle measurement, the uncertainty will decrease accordingly. We show that we can use muon tracks down to a momentum of $3\ \text{GeV}/c$, the lowest trigger threshold for muons. This will provide a large sample of muon tracks for this measurement. Since the central rings require displaced vertices, more integrated luminosity will be needed to achieve the same accuracy as for the other modules. Here it could be considered to use high quality hadron tracks in addition to muon tracks to increase statistics. Furthermore we prove that the absolute accuracy of the measurement does not depend on the amplitude of the Lorentz angle. Thus, this provides a method to monitor the Lorentz angle for the barrel pixel detector throughout its lifetime. We demonstrate that even an input Lorentz angle wrong by 20% in the pixel hit reconstruction does not bias the result. Additional tests show that the impact of misalignment in the startup phase of the CMS detector is negligible, not increasing the uncertainty of the Lorentz angle measurement.

Once the pixel detector is highly irradiated the electric field will no longer be uniform. An alternative method for offline hit reconstruction will then be used, where the Lorentz angle does not have to be known [7]. For high level trigger reconstruction [8], an effective Lorentz angle will be used, taking the electric field to be constant. Alternatively, the correct shape of the Lorentz drift as a function of the charge carriers production depth could be used in a modified hit reconstruction. This would result in a more precise hit position estimate for highly irradiated sensors compared to the approach using an effective Lorentz angle.

References

- [1] Y. Allkofer, et al., Design and performance of the silicon sensors for the CMS barrel pixel detector, Nucl. Instrum. Meth. A584 (2008) 25–41.
- [2] A. Dorokhov, et al., Tests of silicon sensors for the CMS pixel detector, Nucl. Instrum. Meth. A530 (2004) 71–76.
- [3] A. Dorokhov, et al., Electric field measurement in heavily irradiated pixel sensors, Nucl. Instrum. Meth. A560 (2006) 112–117.
- [4] CMS Collaboration, The CMS Technical Design Report, Vol. 1: Detector Performance and Software CERN/LHCC 2006-001.
- [5] B. Henrich, R. Kaufmann, Lorentz-angle in irradiated silicon, Nucl. Instrum. Meth. A477 (2002) 304–307.
- [6] E. James, Y. Maravin, M. Mulders, N. Neumeister, Muon identification in CMS, CMS Note 2006/010.
- [7] M. Swartz, D. Fehling, G. Giurgiu, P. Maksimovic, V. Chiochia, A new technique for the reconstruction, validation, and simulation of hits in the CMS pixel detector, CMS Note 2007/033.
- [8] CMS Collaboration, The TriDAS Project Technical Design Report, Vol. 2: Data Acquisition and High-Level Trigger CERN/LHCC 2002-026.